

# Geoid, its Temporal Variation and Dynamic Topography as Constraints in Global Geodynamics

Frankfurt, 27.09.2004

K. Niehuus, H. Schmeling

K. Niehuus, e-mail: [niehuus@geophysik.uni-frankfurt.de](mailto:niehuus@geophysik.uni-frankfurt.de)

Institut für Meteorologie und Geophysik,  
J.W. Goethe Universität Frankfurt a.M.



# Motivation

- Density distributions derived from highly resolved seismic tomography and viscosity models of Earth's mantle are investigated in analytical flow models in order to fit the models' predicted observables to the GRACE satellite-mission's gravity and geoid measurements and to reproduce estimates of dynamic topography as an additional constraint.
- Advection of a given density distribution yields temporal variations of observed quantities. We investigate whether identifiers of such mantledynamic processes may be discerned from other signals contained in GRACE-data.



# Advection of Mantle Density Heterogeneities

- assume density anomalies to be of purely thermal origin

$$\frac{\partial \rho}{\rho_0} = -\alpha \partial T$$

- general equation of heat transfer

$$\rho C_p \frac{\partial T}{\partial t} = -\rho C_p \mathbf{v} \cdot (\nabla T - \nabla T_s) + \tau \epsilon + K \nabla^2 T + A$$

$C_p$  heat capacity at constant pressure,  $\nabla^2 T_s$  adiabatic temperature gradient,  $\epsilon$  strain tensor,  $K$  constant thermal conductivity,  $A$  heat production

- neglect viscous dissipation, heat conduction, heat production as minor effects. Density change is now only due to advection,  $\alpha \rho_0$  is constant with depth

$$\frac{\partial \delta \rho}{\partial t} = -\nabla \delta \rho \cdot \mathbf{v}$$



# Modeling Dynamic Observables

- Literature provides a constant or depth-dependent linear relationship  $\rho_{lm}(r) = \frac{\partial \ln \rho}{\partial \ln v_{s/p}} \left( \frac{\delta v_{s/p}}{v_{s/p}} \right)_{lm} \rho$  between relative thermally induced density and seismic velocity anomalies from tomography where  $\frac{\partial \ln \rho}{\partial \ln v_{s/p}}$  is the scaling factor  $c$ .
- Our flow models employ a selection of s-wave seismic tomographies: (1) mk12wm13s, (2) ngrand, (3) s20a, (4) s20rts, (5) s362d1, (6) saw24b16, (7) sb10l18, (8) smean, a weighted average of several models which comprises features common to selected models and deemed robust in the sense of a largest common denominator model (Becker & Boschi, 2002), and (9) smean\_nt with cratons removed (3SMAC, Nataf & Ricard, 1996).
- A second model series replaces tomography-derived densities of the upper mantle by slab sinking model stb00d (Steinberger). The upper mantle scaling factor  $c$  fits the slab-density contrast.



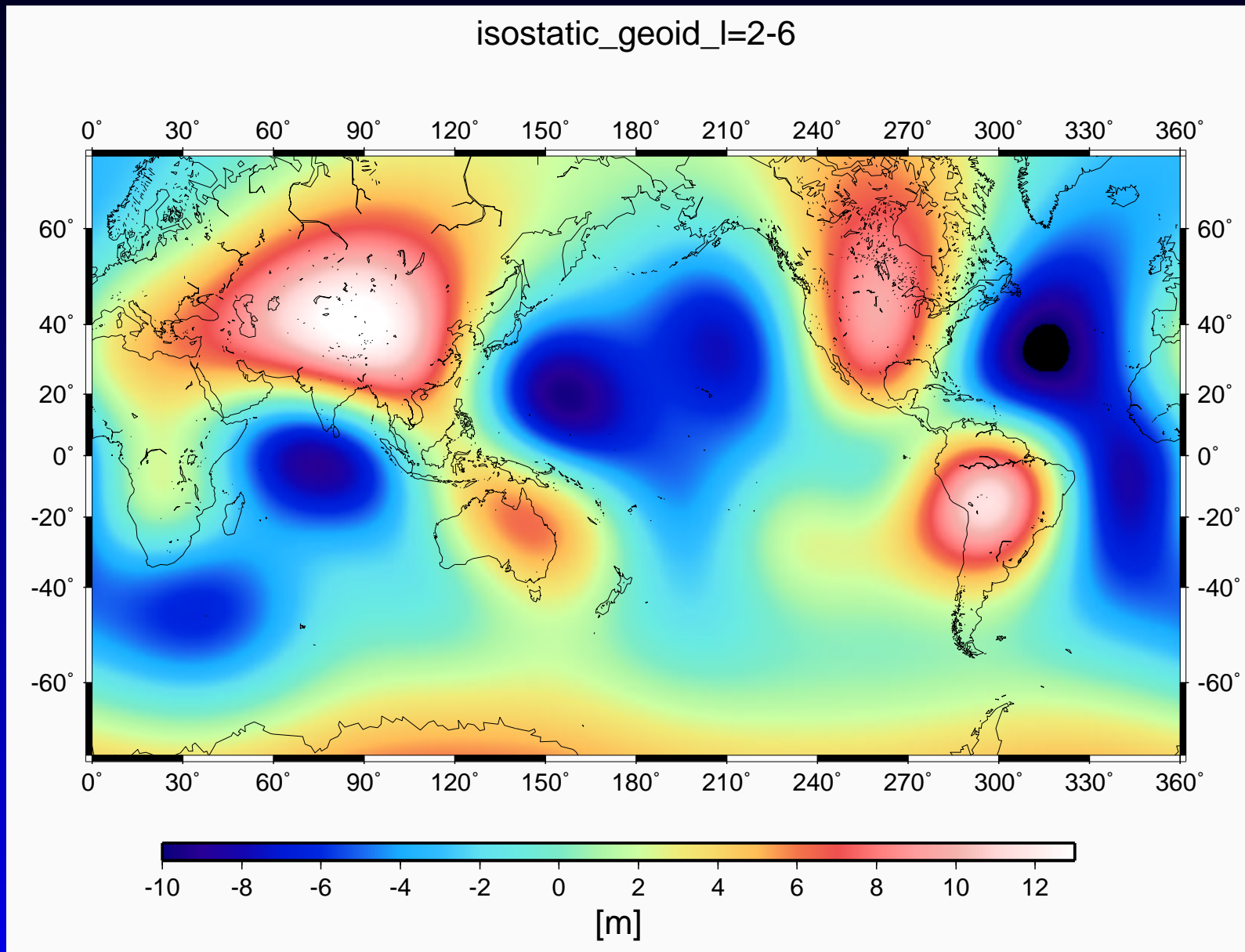
# Fitting

- In a forward Monte-Carlo search comprising about ten million models we chose to fit viscosities and velocity-to-density scaling factors for a radially stratified mantle of 8 layers to the observed non-hydrostatic (Nakiboglu, 1982) dynamic geoid derived from EIGEN-GRACE01S comparing successful models with an estimate of dynamic topography derived from ETOPO5. Both observables are corrected for fields due to isostatically compensated crust, oceanic lithosphere (half-space cooling model) and tectosphere (Panasyuk & Hager, 2000).
- The fitting criterion is the variance reduction, a measure of the minimization of the misfit  $P$  between observed and predicted long-wavelength geoid

$$P(\eta, c)/[\%] = \left[ 1 - \left( \frac{\sum_{l=2}^{max} \sum_{m=-l}^l (\delta N_{lm}^{obs} - \delta N_{lm}^{pred})^2}{\sum_{l=2}^{max} \sum_{m=-l}^l (\delta N_{lm}^{obs})^2} \right) \right] \cdot 100 > 70$$



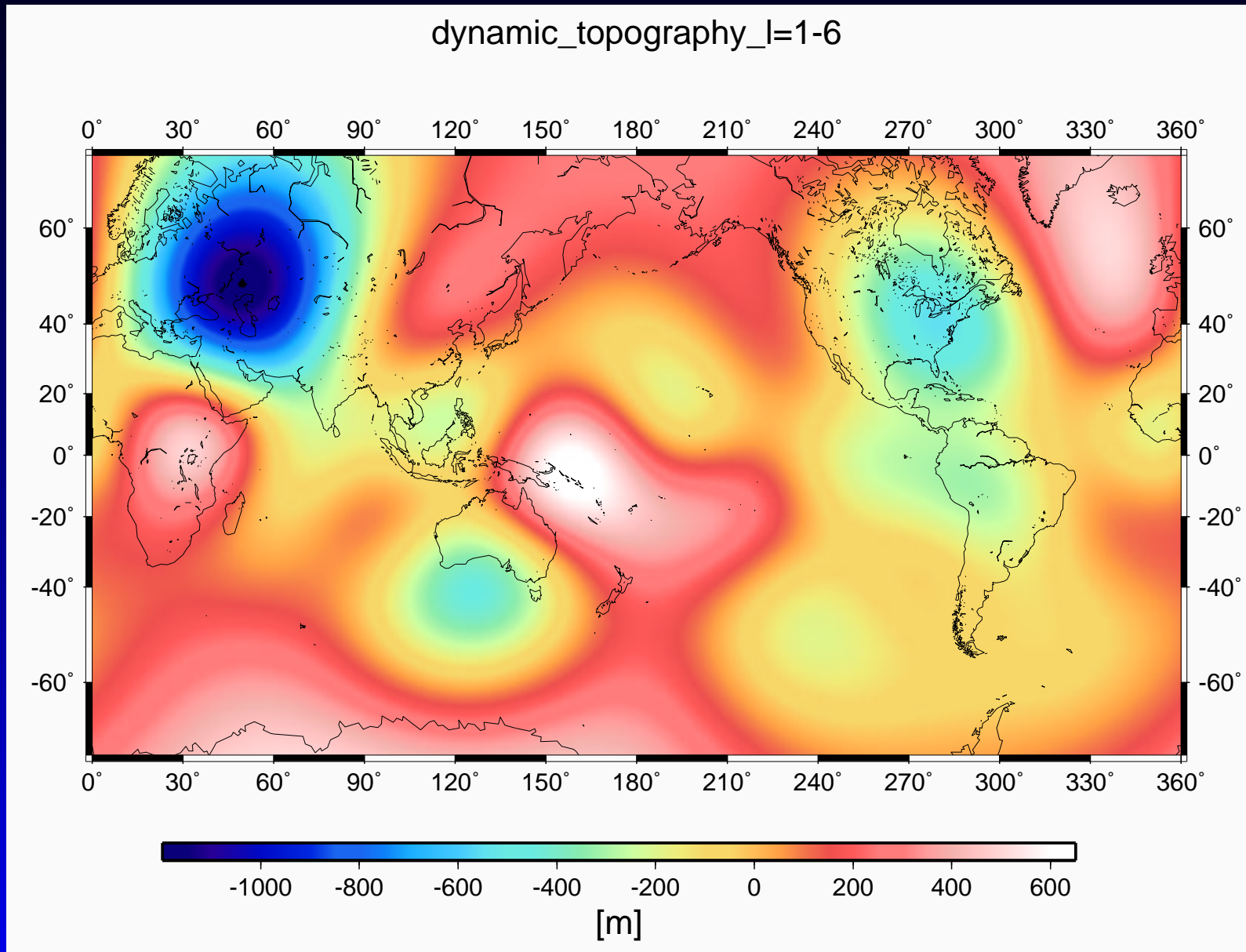
# Isostatic Geoid



(Panasyuk & Hager, 2000).



# Dynamic Topography



(Panasyuk & Hager, 2000).



# Constraint on "Average" Mantle Viscosity

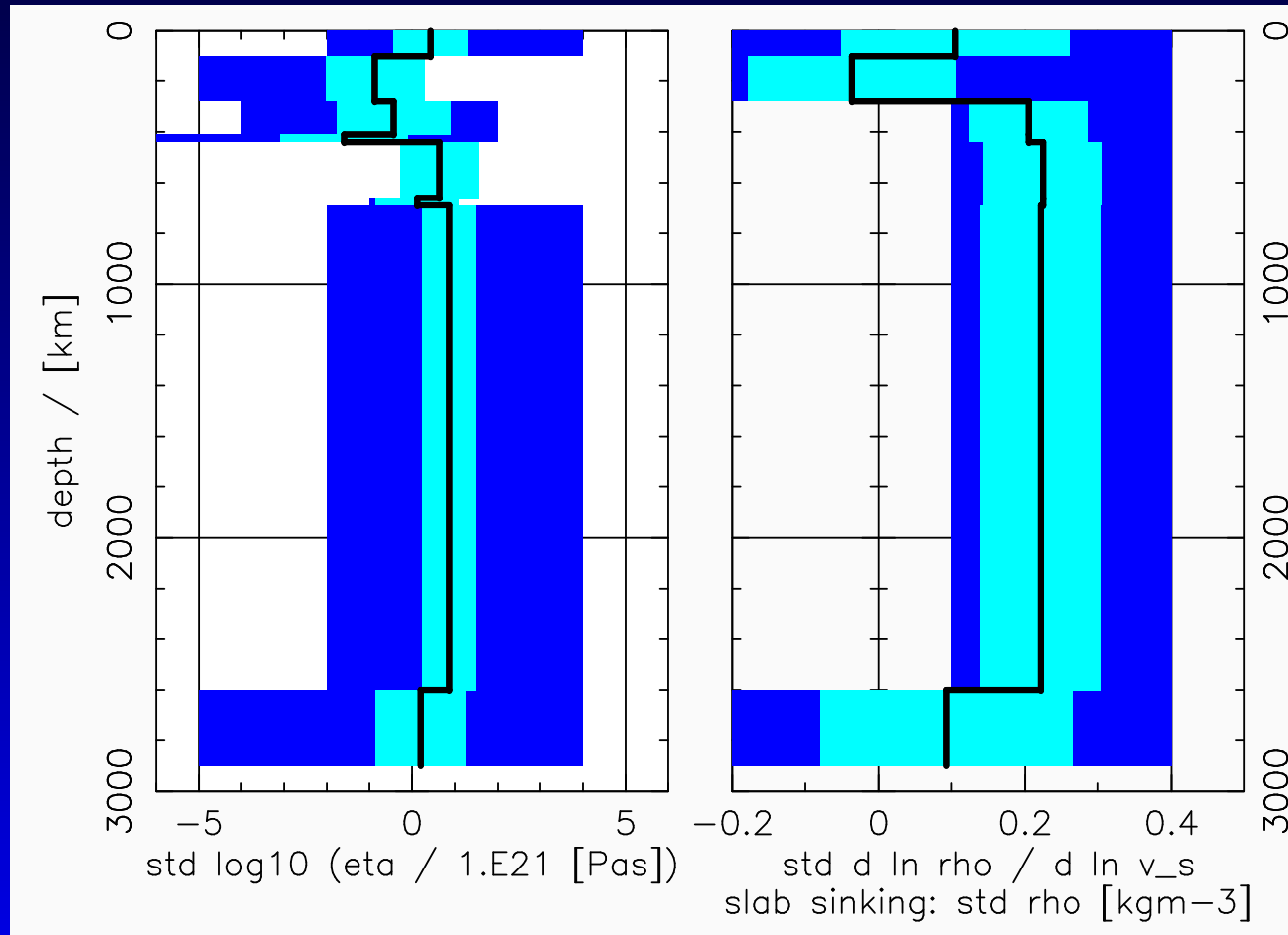
A linear combination of model viscosity values from the base of the lithosphere to a depth of 1400 *km* weighted by sensitivity implied by Angerman River Frechet kernels of appropriate viscosity profile should satisfy an estimated Haskell value of  $0.65E21 - 1.1E21 Pa s$  (Mitrovica, 1996).



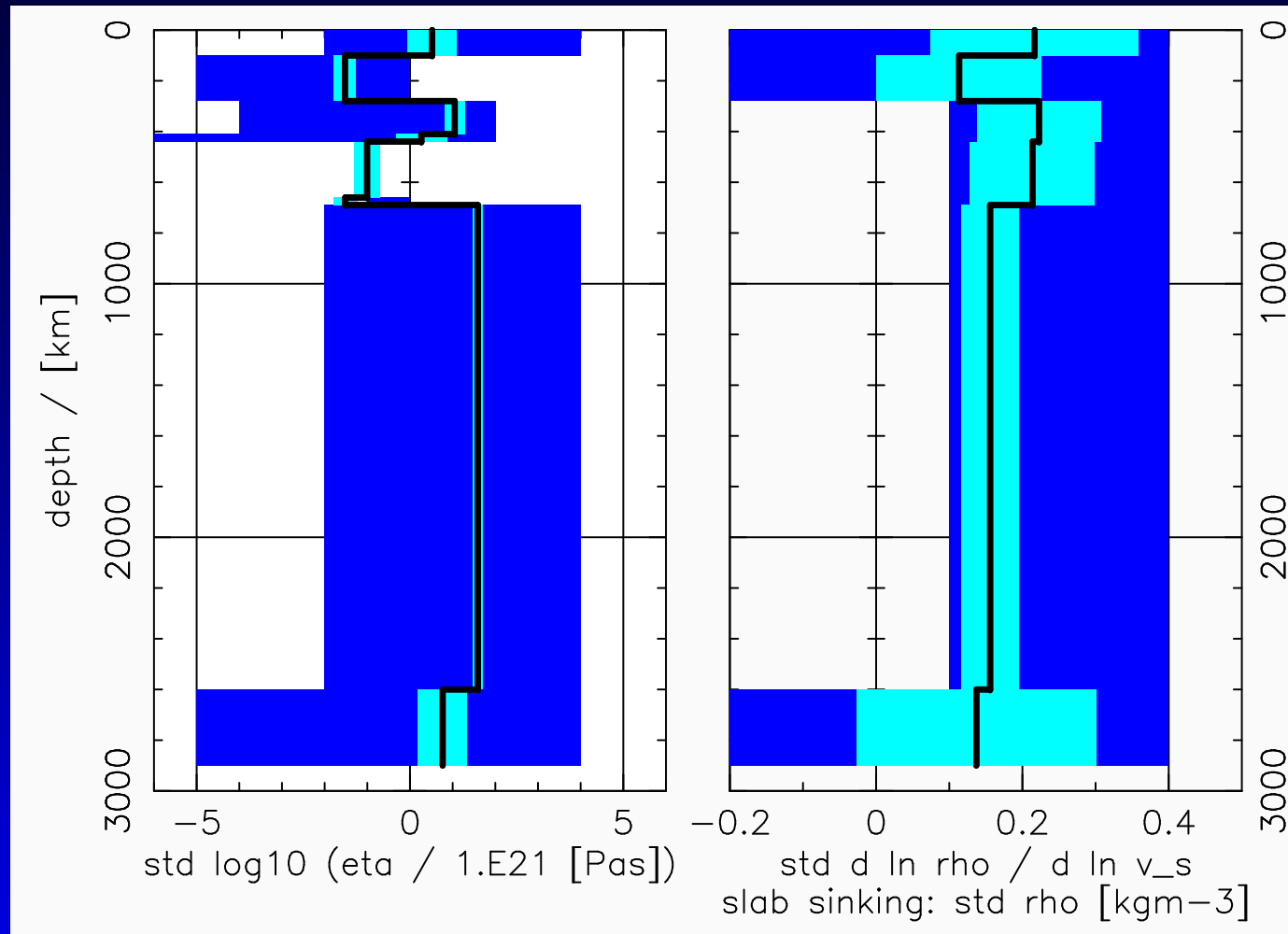


# Solution of Forward Inversion

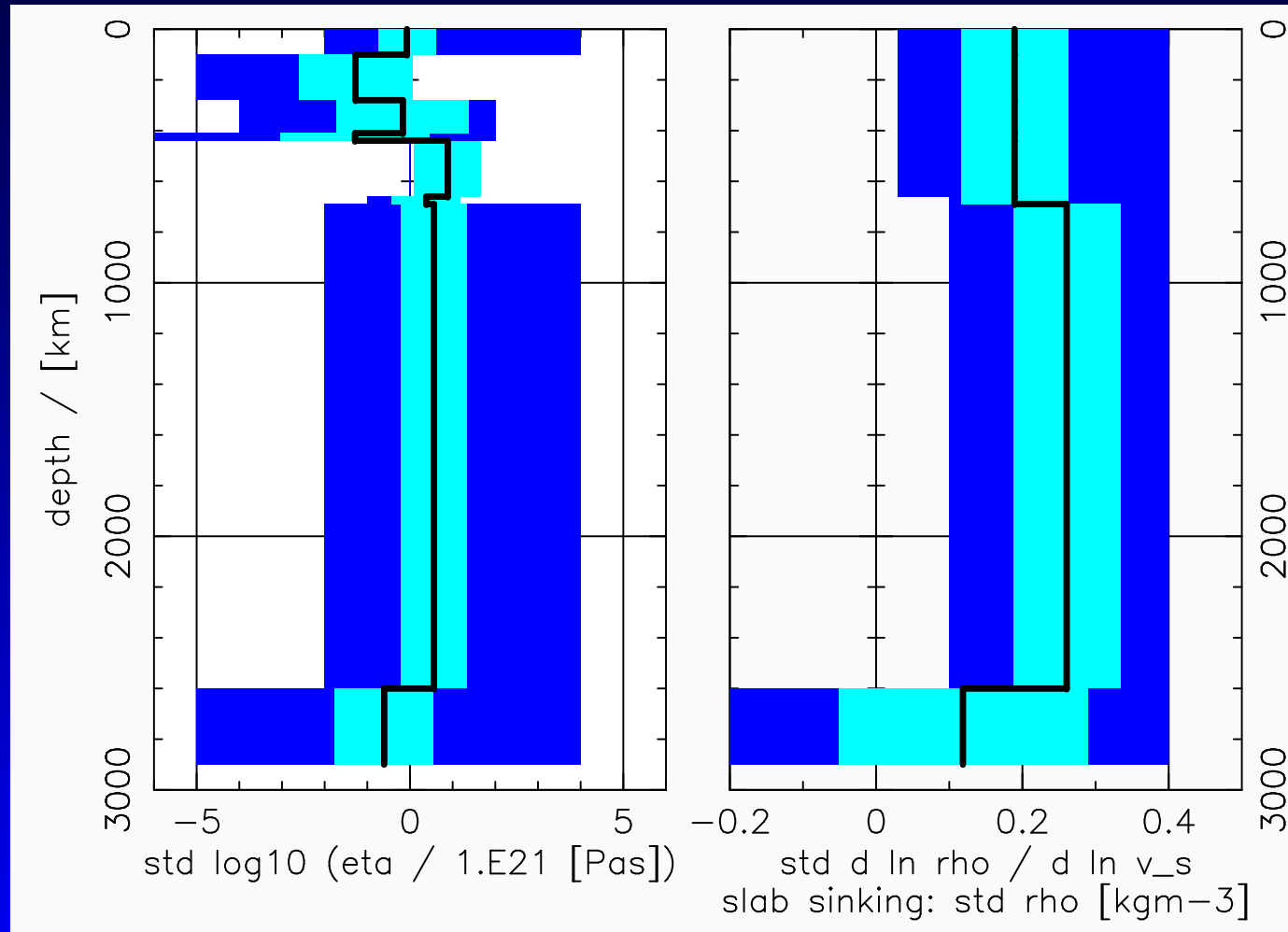
Mean deviation (*light blue*) from mean (*black*) over all successful free-slip models from all 9 seismic tomographies rendering geoid fits above tolerance level ( $P > 70\%$ ).



# Successful kinematic models using smean\_nt-derived mass distributions:

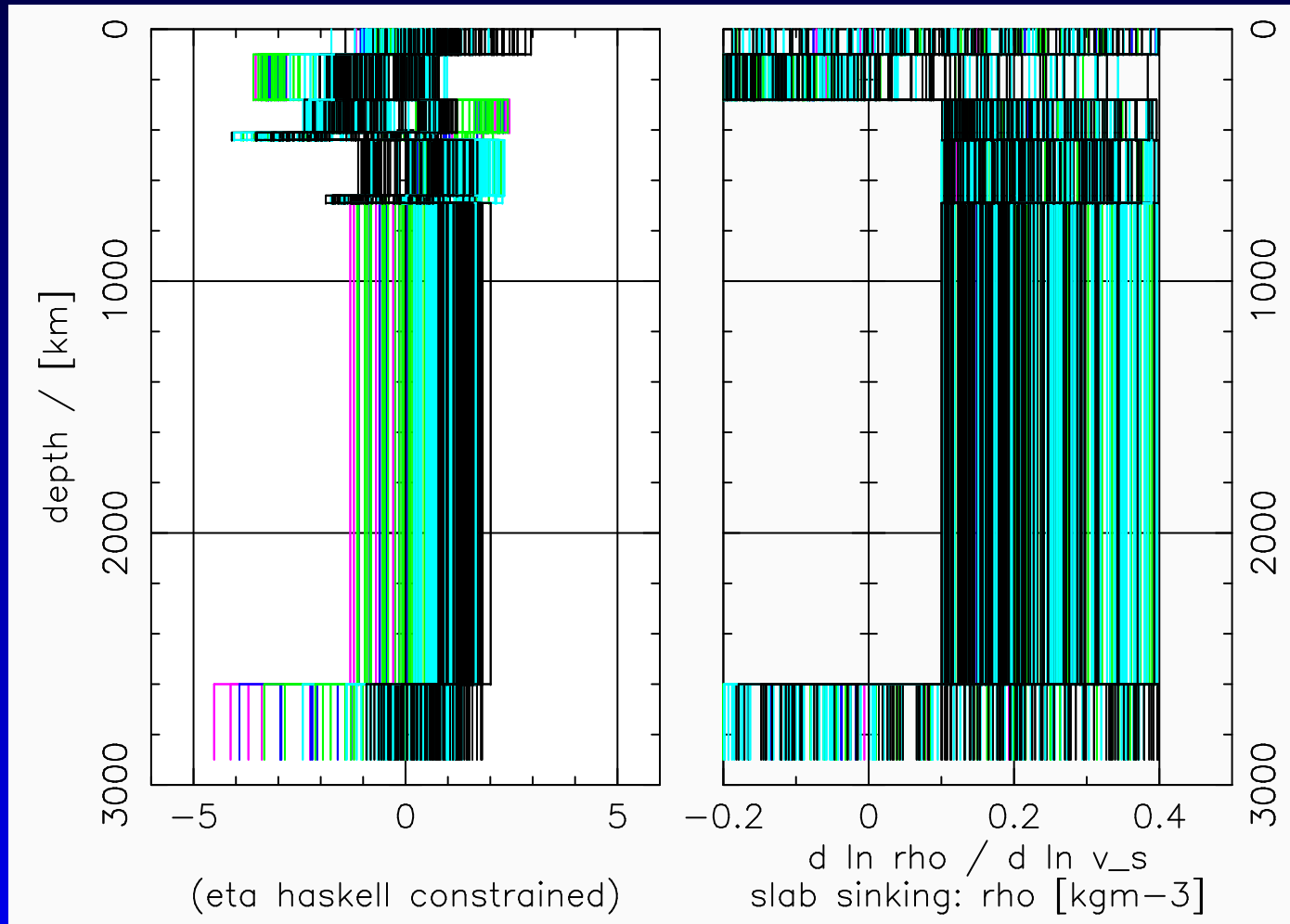


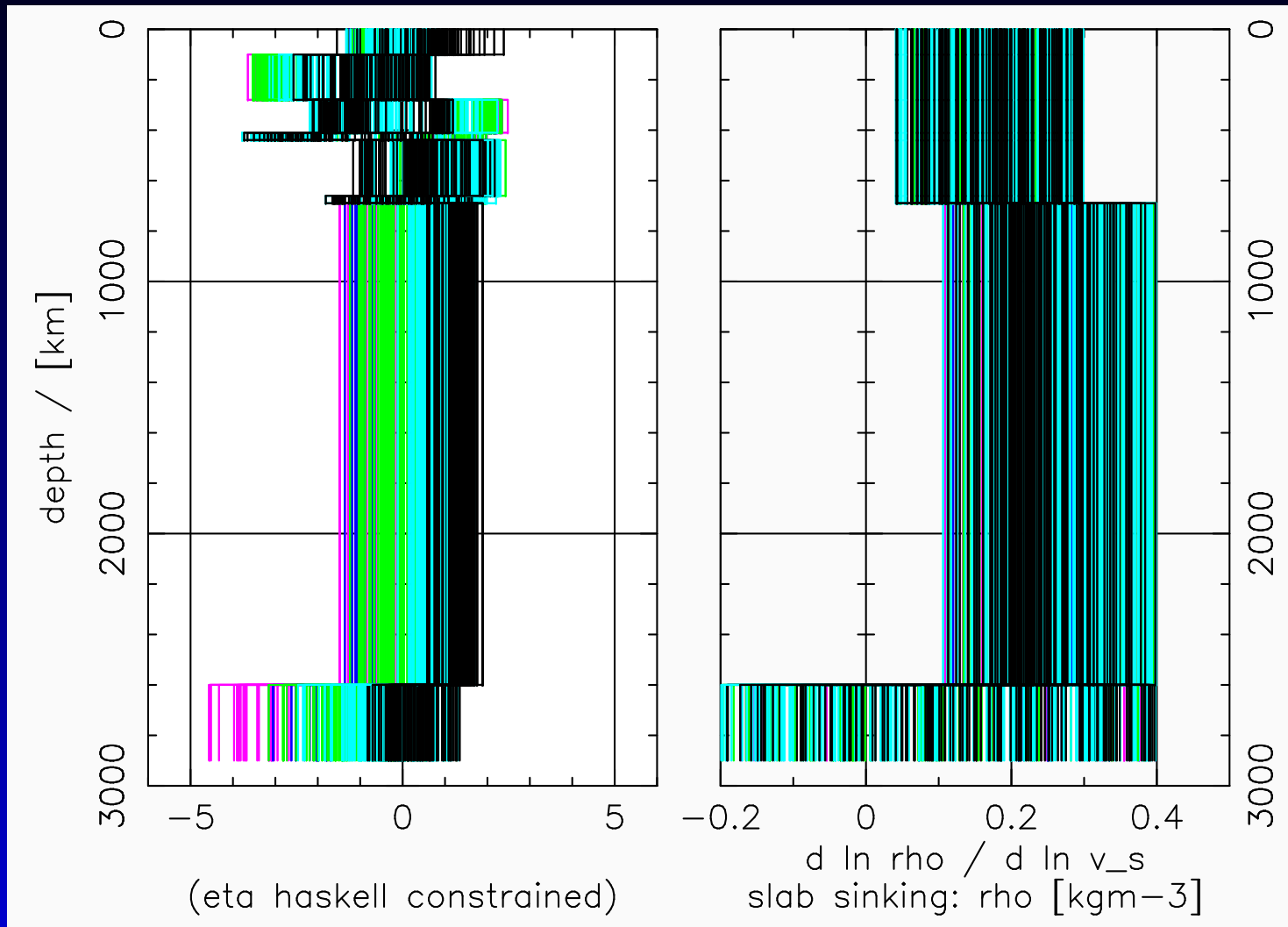
Successful free-slip models with upper mantle tomography-derived mass distributions replaced by slab sinking model (stb00d, Steinberger):



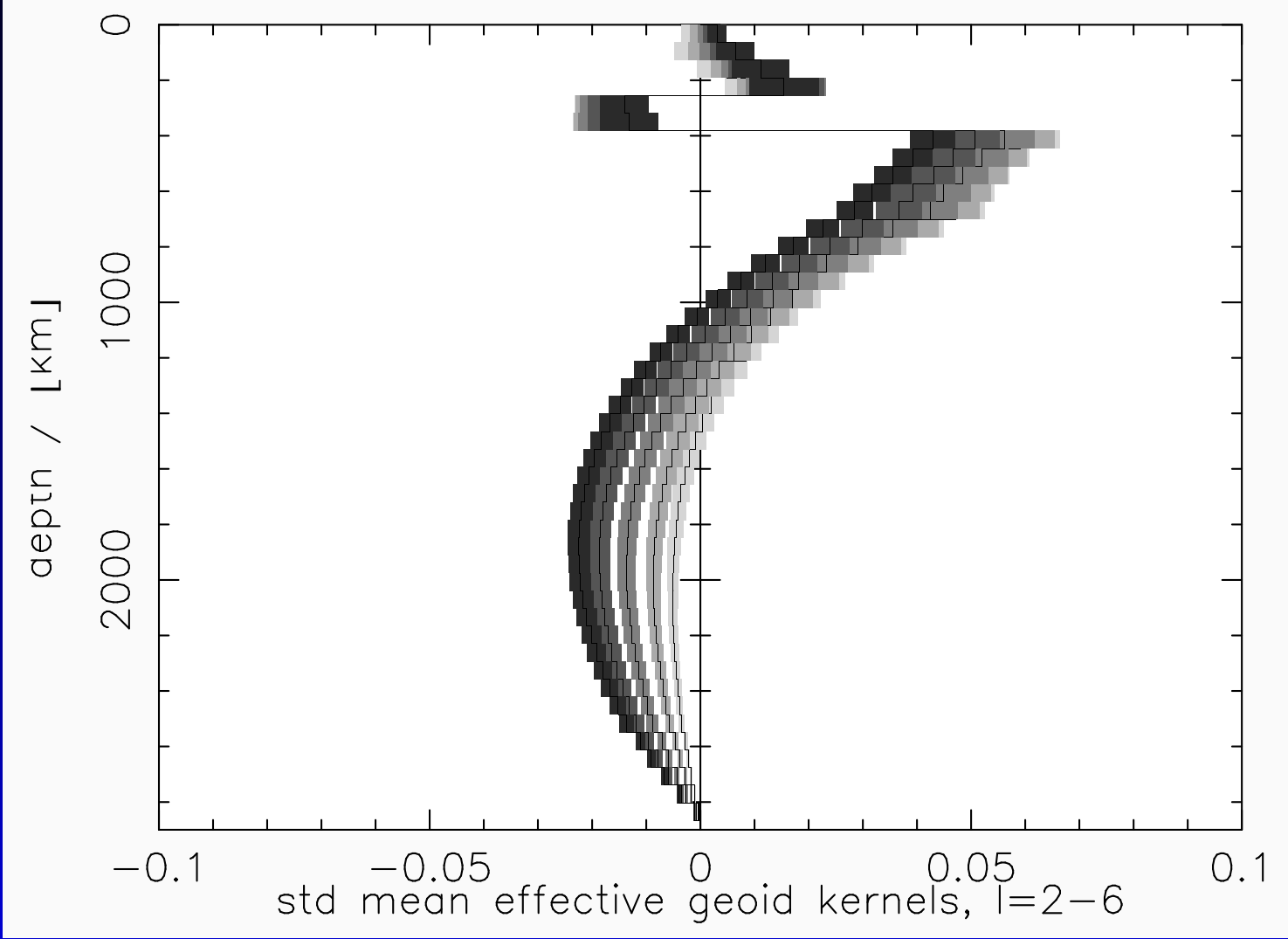
# Temporal Geoid Variations

Color-coded according to spectral power of  $\frac{dN}{dt}$ :  
resolved by GRACE 1-yr (*cyan*) or 5-yr (*green*) mission duration,  
*mm/a* (*dark blue*), *cm/a* or higher (*red*) and unresolved (*black*)

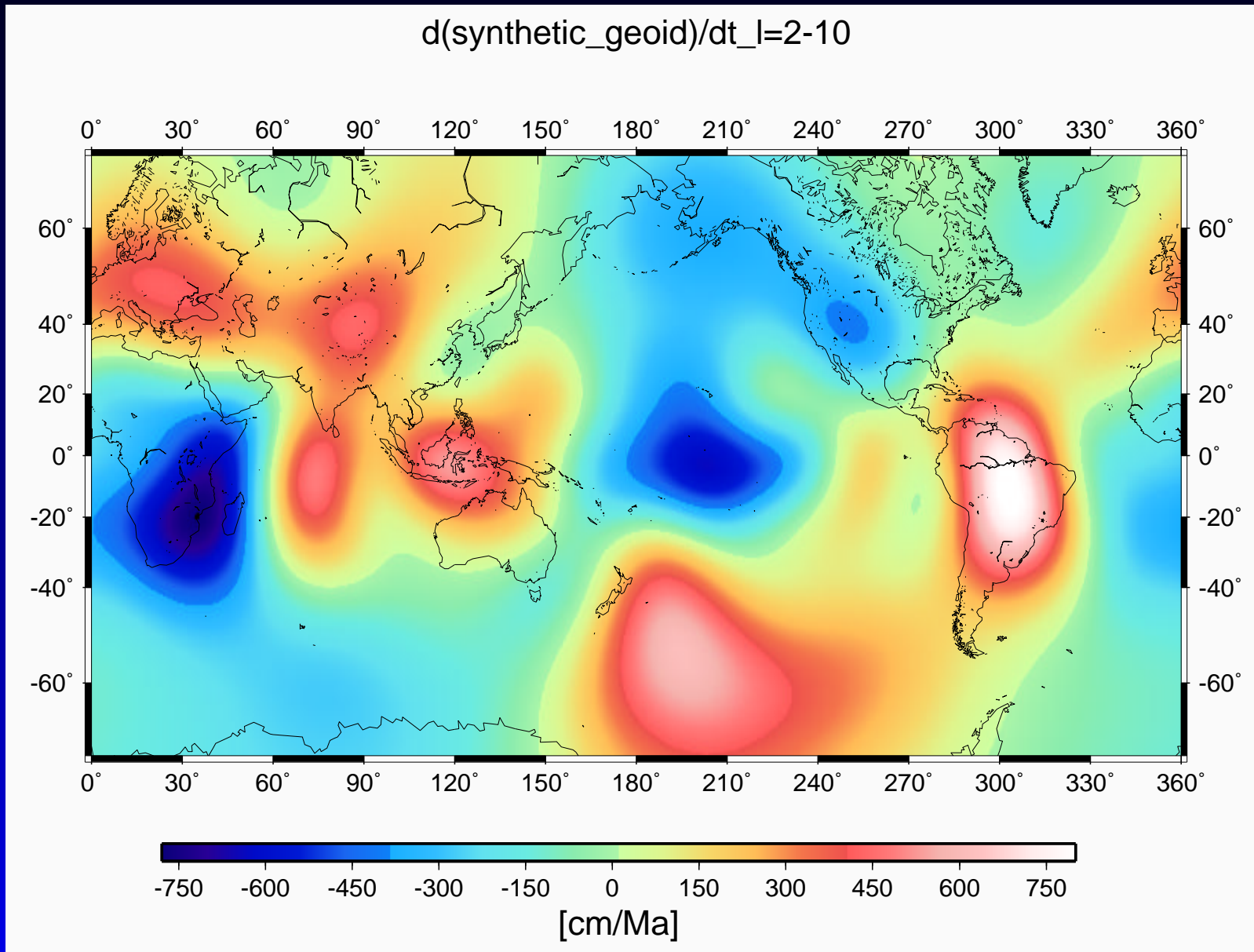




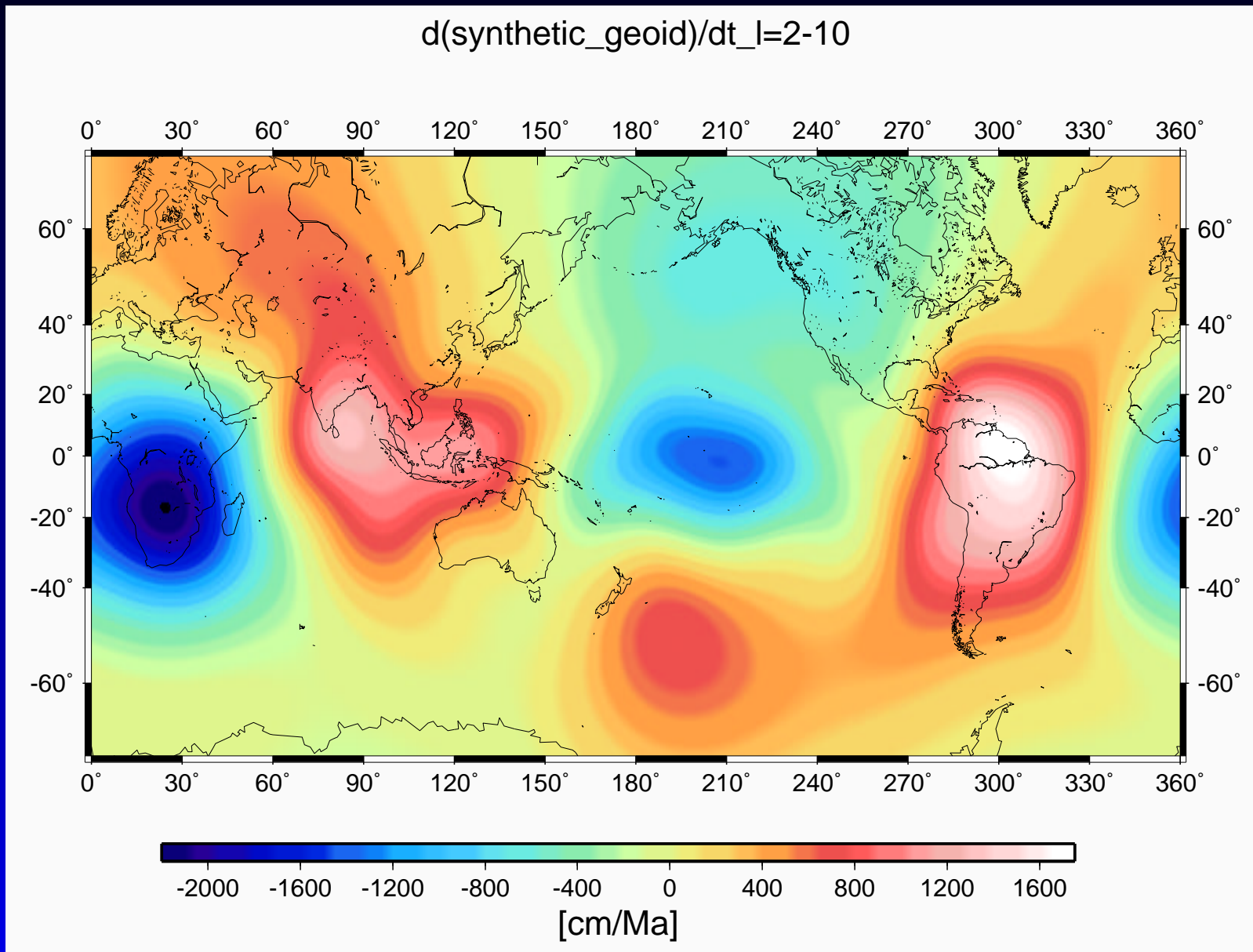
# Mean Effective Geoid Kernels, Free-Slip



# Mean spatial $\frac{dN}{dt}$ , Tomography Models



# Mean spatial $\frac{dN}{dt}$ , Hybrid Models





# Conclusions

- We can identify a distinct family of solutions within our models which may lie within the resolution limits of annual temporal geoid variations of the ongoing GRACE mission.
- However, global geoid variations estimated by advecting density heterogeneities from our likely selection of successful models are small ( $< O(-4)m/a$ ) in comparison to those due to PGR, ocean circulation, redistribution of water and biological masses, or massive volcanic processes ( $O(-3)m/a$ ).



## Problem: Observed Plate Motions

- Free-slip models commonly do not reproduce observed plate motions.
- The problem of reproducing observed plate velocities or incorporating them in the model approach features prominently in many studies and remains largely unresolved. While Zhong & Davies, 1999 consider the inclusion of plate velocities as a surface condition meaningful only in conjunction with laterally strong and weak zones in the lithosphere, a study comparing the effects on the predicted geoid of various methods to mimic plate tectonics such as weak zones, force balance and imposed plate velocities 'moved by the hand of God' conceive the latter method by far the best way to include the effect of plate velocities on the geoid (Karpychev & Fleitout, 1996).
- The much-debated choice of upper surface boundary conditions has a large influence on the mantle flow field and surface observables.



# Problem: Density Distribution

- Global tomography of uppermost regions is not well resolved, seismic anomalies situated shallow, in phase transition regions or near the CMB are partly compositional. Models where upper mantle density heterogeneity is deduced from slab sinking models, however, do not alter fit significantly.
- Uncertainty of tomography-derived density distributions and the aforementioned problem of incorporating realistic upper boundary conditions is likely to cause a flow-field which may yield unrealistic temporal variations of surface observables.



## Next Step

Incorporation of lateral viscosity variations into our models.

- Lateral viscosity variations clearly improve fit to estimated dynamic topography and yield geoid misfits of 88% (Cadek & Fleitout, 2003). Zhang & Christensen, 1993 showed that for a radially stratified viscous mantle with viscosities increasing from upper to lower mantle, LVV may significantly alter the higher harmonics of the geoid ( $l \geq 3$ ).
- The anticorrelation (see also Cadek & Fleitout, 1999) of synthetic topography with the estimated most prominent low over central Eurasia and the dynamically depressed eastern North America disappear when introducing lateral viscosity variations (Cadek & Fleitout, 2003)

